Water Uptake and Interfacial Structural Changes of Thin Film Nafion® Membranes Measured by Neutron Reflectivity for PEM Fuel Cells

V. S. Murthi[a, b], J. A. Dura[b], S. Satija[b] and C. F. Majkrzak[b]

[a] Department of Materials Science and Engineering, University of Maryland, College Park, Maryland 20742, USA
[b] NIST Center for Neutron Research, National Institute of Standards and Technology, Gaithersburg, Maryland 20899, USA

Nafion thin films (~500 Å) spin coated onto the Pt and Au layers on Si are investigated for water uptake and swelling. Neutron Reflectometry data demonstrate that these structures are composed of nafion layers which differ from their bulk properties in terms of their scattering length density and water uptake. However, as the relative humidity is increased, the amount of water in the layers increases for a Nafion on Au and is comparable to that observed on bulk nafion membranes only up to 80 % RH. However, the Nafion on Pt reaches complete hydration at 96% RH. Although, a single layer model was able to fit the NR data obtained on nafion under vapor conditions, only a bilayer model, with an outer less hydrated nafion and an inner more hydrated nafion layer, was able to fit the data in liquid water.

Introduction

Proton exchange membrane fuel cells (PEMFC) with their higher efficiency, low heat and noise signature, fuel flexibility, continuous operation, and modularity are an attractive choice over competitors such as batteries and internal combustion engines for portable and standalone power generation. It is well known that, in order for the technology to become commercially viable, the cost of production of the components in a fuel cell must be reduced and, more importantly, the durability and the life time of the MEA must be improved. In this context the role of the polymer electrolyte-electrode interface is crucial, being at the core of the energy conversion process. At this interface efficient transport of ions, dissolved reactants (such as O_2, H_2 and gases from reformate) and products as well as electrons have to be maintained for sustaining high-current densities without reaching mass transport limitations early on.

Nafion, the current benchmark proton exchange membrane (PEM) fuel cells, exhibits good thermal and chemical stability as well as high proton conductivity under hydrated conditions at temperatures below 90°C. However, applications of these membranes are limited at high temperatures and low relative humidity (RH) due to their loss of conductivity. Although lower RH operation offers quicker start-ups and better freeze-cycle management, the mechanism of degradation is an especially important research topic for the ionomer membranes, because this may lead to gas crossover, local membrane breakdown or thinning, lowering of catalyst utilization in the membrane electrode assembly (MEA), and the mechanism elucidation would lead to effective means for the longevity of fuel cells.1-3.

There is an increasing awareness that events such as start-up and shutdown, oxidant starvation, transitions to lower relative humidity and overpotential (under conditions of variable load and fuel starvation) can severely effect the lifetime of perfluorinated

membranes. Because these variables are closer to actual commercial operation, their relevance cannot be overemphasized. Several recent publications have pointed to serious interfacial degradation, most notably those where morphological changes to the membrane electrode assemblies are reported including dissolution of Pt[1] and alloying elements[2, 3] (from the cathode), and associate changes in membrane degradation as well as irreversible changes to the reaction layer (catalyst layer), including catalyst migration and loss of hydrophobicity in the reaction zone.

Membrane structural properties and durability continues to be an area of interest that has not seen considerable improvement mainly because of the limited spectroscopic techniques available to study catalyst-MEA interfaces in a working fuel cell. Recently, Neutron Imaging has been used successfully to monitor the water transport gradients within Nafion inside a working fuel cell.[4-7] Several studies to reveal the structure of Nafion membranes using small angle scattering have suggested various kinds of structure like lamellae, core-shell, sphere, cylinder, fibrils, etc.[8-12] Dynamics of water in the perfluorosulfonic acid membranes have also been studied using quasi elastic neutron scattering (QENS).[13, 14] There have also been attempts using infrared spectroscopy[15-17] and NMR[18-20] to study the water-ionic domain interaction. Proton conductivity of Nafion membranes depends on relative humidity (RH), diffusion coefficient, water uptake and temperature. Therefore, monitoring the water sorption within the membrane framework is important to understand the sorption behavior and proton conductivity of Nafion membranes. There have been numerous publications using small angle neutron scattering to study water domains in Nafion.[21, 22] Recently, Kim *et. al*. measured the vapor sorption for a series of Nafion 1100 membranes (as received and pretreated) using Small Angle Neutron Scattering (SANS).[23] They found strong correlation between the interionic domain distance and water uptake indicating that the matrix structure changes due to the mobility of the main chain even at room temperature. The objective of our study is to understand the water uptake and structural changes of the Nafion-water interface. We employ a model system of the films of nafion on thin film metallic surfaces based on the requirements of Neutron Reflectometry (NR). Understanding the nature of the Nafion structure that is vulnerable to degradation is of great interest, not only from the point of technologies made available by recast Nafion membranes, but also to mimic and isolate the Nafion interfaces in the catalyst layer of the MEA. In our current scope of measurements, water sorption isotherms and the corresponding structural properties of Nafion membranes spin-coated on smooth gold and platinum surfaces are compared.

Neutron Reflectivity: Theory and Background

Neutron Reflectometry, NR, is a well established technique for studying the composition of thin films and layered structures on a nanometer scale. The intensity of neutron beam reflected as a function of the glancing angle from a flat surface depends upon the composition and structure of the underlying matter. Using NR, films as thin as 1-2 nanometers can be measured with sub-Angstrom resolution.[24] The scattering length density, ρ, (SLD) is a sum of the product of the number density (N_i) of the isotopes in a material, times the scattering length (b) of the isotope, and therefore the SLD profile can also readily provide a composition depth profile when the constituents are known. Based on NR fitting, both SLD profiles and the surface roughness can be determined. NR provides major advantage over X-ray and electron beam techniques not only in its ability to penetrate bulky samples but also because of its non-destructive nature and the

sensitivity with which it can distinguish between hydrogen and its isotope, namely deuterium. For example, the SLD of D_2O is 3.2028 x 10^{-4} and H_2O is -2.8143 x 10^{-5} Å^{-2} (a factor of ~12 difference). Because the SLD is not proportional to the atomic number Z as in x-ray or electron based techniques, one of the main advantages of neutron reflectometry is its ability to discriminate isotopes or different compounds with similar average electron density.[25]

Specular reflectivity is defined as the reflected intensity divided by the incident intensity as a function of the wave vector, $Q_z=4\pi\sin\theta/\lambda$, where θ, the angle of incidence is equal to the angle of reflection as shown in Figure 1a. By changing the angle of incidence relative to the sample surface, information about the in plane structure can be determined. The critical edge, as shown in Figure 1b, is defined as the angle below which neutrons are totally externally reflected (100% reflectivity) and is a function of the SLD according to equation 1:

$$k_c = 4\sqrt{\rho\pi} \qquad [1]$$

where, k_c is the critical wave-vector transfer and ρ is the SLD.

Beyond the critical angle, the period of oscillation of the reflected intensity is inversely proportional to the thickness of the layer. Figure 1b illustrates the reflectivity curve on a 500 Å Nafion thin film on a 50 Å Pt/Si substrate film. The periodicity in the Q-value of reflected intensity maxima is determined by the SLD of the film. The reflected intensity generally decreases as Q_z^{-4}. However, if the sample consists of more than one interface the reflected intensity shows an interference pattern superimposed on the rapidly decreasing function. This is because successive interfaces at different depths give rise to reflected beams which interfere constructively or destructively with each other at different angles of incidence. NR data of samples can then be fit to a model consisting of several layers of thin films of varying SLD, thickness and roughness. From simultaneous fitting of all the parameters a profile of the sample structure can be arrived.

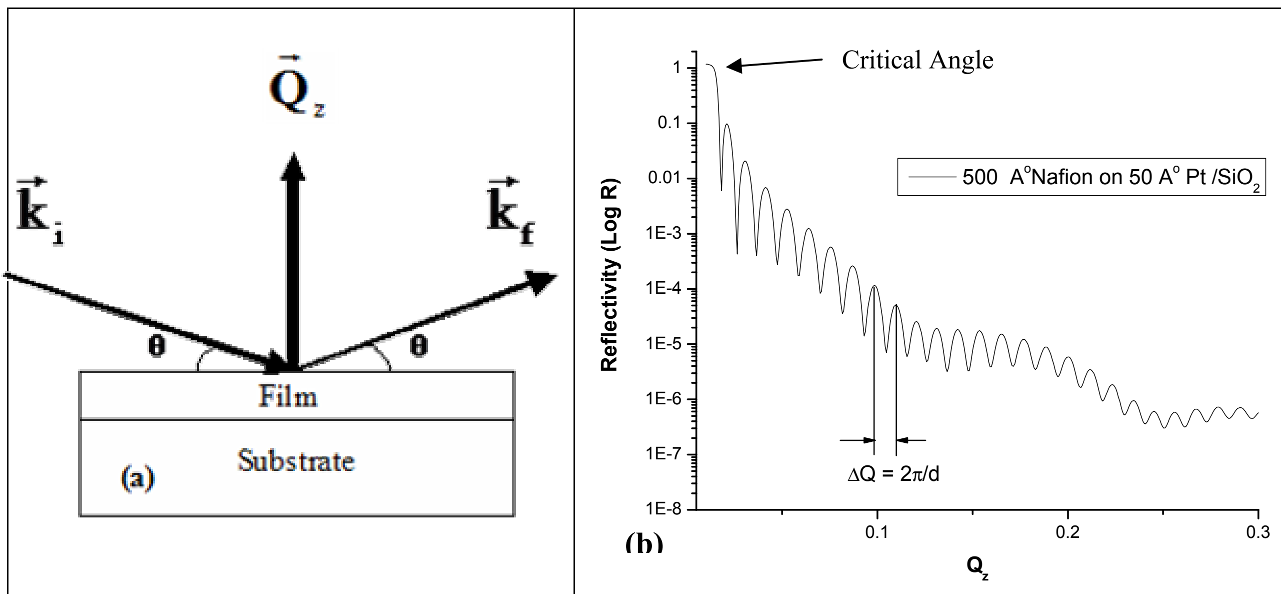

Figure 1. **(a) Schematic of a single layer NR experiment showing basic principles and (b) reflectivity profile for a film/substrate system, here, 50 Å Pt/Si.**

Experimental*

Substrate Preparation:

The most important requirement for any NR experiment is that the substrate should be as smooth as possible with none or very low surface roughness. Silicon wafers make very good substrate materials due to their ~5 Å surface roughness and provide a platform to study deposited films (both metal and polymer thin films). Si (100) wafers (~ 5Å surface roughness) were used in all our measurements. They were cleaned using detergent and sulfuric acid mixed with nochromix to remove contaminants prior to magnetron sputtering deposition of a 20 Å Cr adhesion layer followed by a 140 Å Au or 60 Å Pt as the case may be. The base substrates containing Au-Cr or Pt were first characterized by x-ray reflectivity measurements for an independent determination of the film thickness and roughness.

Nafion Film Preparation:

A 5 wt% Nafion® 1100 equivalent weights (EW) was further diluted 16 times with 99% ethanol. This solution was then used to spin coat the Au-Cr or Pt coated Si substrates using a Headway Research Inc.* spinner (model PWM 202) with digital speed controller. A shaft rotation of 3500 rpm and 30 seconds were chosen to yield Nafion films in the range 450 – 550 Å. All films were then heat cured to 60 °C in a vacuum oven for 1 hr. Although this article focuses entirely on Nafion films heat treated at 60 °C, NR was also performed to measure the water uptake as a function of thickness of Nafion and at curing temperature (150 °C). Water uptake as a function of annealing temperature, thickness and kinetics of water sorption is beyond the scope of this article.

Sample Environment:

For Nafion film samples exposed to H_2O vapor at various %RH, a special sample chamber was constructed of Al and had ports for gas inlet and outlet, RH probe, thermocouple and a sample stage made of copper with separate inlet and outlet through which a coolant or heated liquid could be circulated. Once the sample was mounted inside the Al chamber, it was sealed off and ready to be used for NR measurements. Argon, the carrier gas, was flowed through a LI-COR (610-01) humidity generator at typical flow rates of 0.5-2 SCFH into the Al chamber and allowed to reach equilibrium. Since neutron transmit through Al with little or no attenuation, the sample alignment and NR measurements were then done under varying conditions of humidity. During data collection the sample was kept constant within ~0.5°C, measured by a Pt resistor on the heat sink. The relative humidity was monitored using a Viasala RH probe, although all reported values in this article are determined from the sample temperature and dew point. Further, Si substrates (76.4mm diameter) that are 5mm thick were used so that the clamping would not warp the sample.

In this work, water sorption isotherms (or water uptake) based on neutron reflectivity (NR) measurements are reported for Nafion thin films deposited on a Au-Cr/Si and Pt/Si substrate as well as their respective water uptake from liquid H_2O. For the measurements in liquid water, a special cell was used as detailed in a previous publication.[26] Briefly, the sample is sandwiched between silicon wafers with the provision of gaskets in between

that minimizes the amount of solvent held in contact with the sample surface – reducing it to a layer 100 μm thick. The solvent in this reservoir can be flowed from the outside allowing easy replacement of the aqueous buffer without disassembly of the cell.

Neutron Reflectometry:

The neutron reflectometry data were taken using the Advanced Neutron Diffractometer/Reflectometer (AND/R) at the NIST Center for Neutron Research. A description of the instrument can be found in the literature. The specularly reflected intensity was measured as a function of incident angle between the range $1° < 2\theta < 14°$. The two slits (slit numbers 1 and 2) upstream of the sample as shown in the Figure 2 were opened continuously in proportion to θ in order to provide a constant $\Delta Q/Q = 0.025$, and a constant projection of the beam 1.7 inches wide on the plane of the sample. Two slits downstream of the sample (slits 3 and 4) were used to minimize background scattering into the detector. They were also opened in proportion to θ, at widths determined sufficient to admit the entire specularly reflected beam into the detector. The background scattering was measured in two sets of scans in which θ was offset to 3/8 and 5/8 of 2θ, values determined to be off the specular ridge by measuring rocking curves on similar samples. The background was subtracted from the specularly reflected intensity and this result was normalized by a slit scan to yield, R(Q), the reflectivity as a function of Q.

Both the data reduction and analysis was performed using the Reflpak software[27] developed at the National Institute of Standards and Technology, Gaithersburg, MD using the matrix formalism of Parrat.[28] The input to the program is the observed reflectivity data, R(Q), and an initial trial layer profile for least-squares fitting.

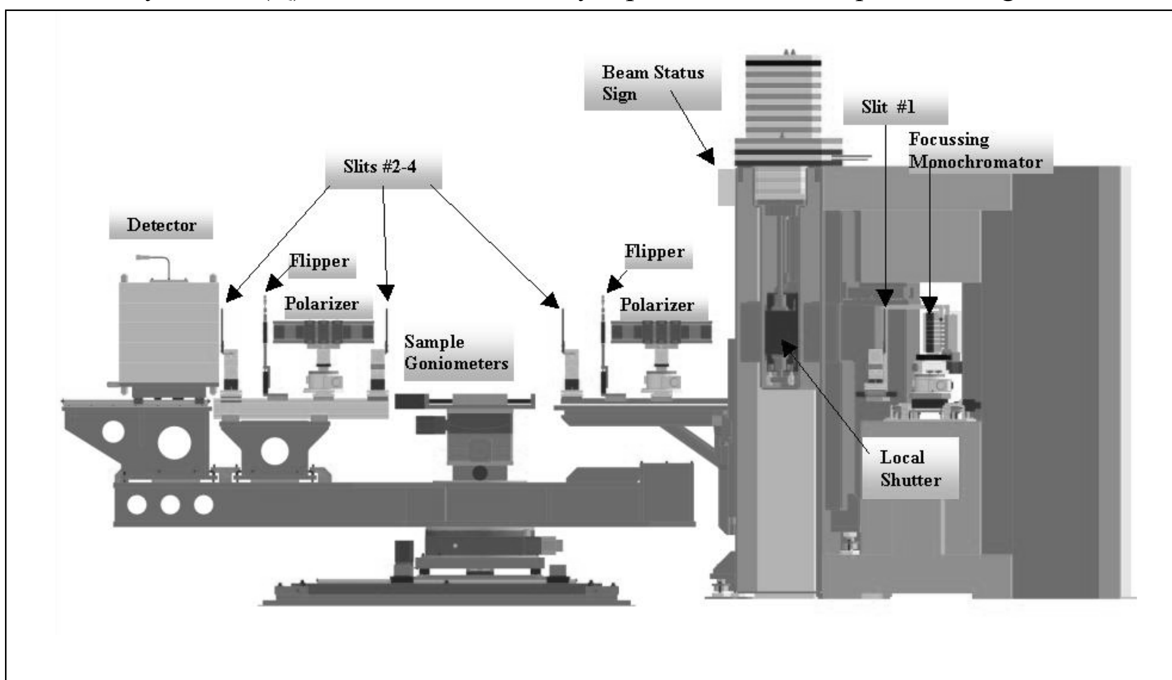

Figure 2. View of the AND/R instrument at the NCNR showing the major components for beam operation. Additional components such as the Flipper and polarizer also shown.[29]

The layer profile models the sample as a series of layers, each having a constant ρ and thickness d. Both ρ and d of a layer are adjustable parameters, and the user can include as many layers as necessary in order to accurately model the sample. Rough interfaces between layers are modeled as a series of individual layers with an error function (erf) of ρ between the two media over a given distance which also is an adjustable parameter. Thus the program is capable of modeling very general layer profiles, and the responsibility is on the user to ensure that the derived profiles are physically meaningful. In this article all SLD are represented as 16πNb $Å^{-2}$ units.

Results and Discussion

Neutron reflectivity data as a function of relative humidity (% RH) from a nafion film deposited on a gold-chromium on Si substrate is plotted in Figure 3. The calculated SLD, ρ, for dry nafion containing one proton is 2.0925 x 10^{-4} (16*π* 4.1628 x10^{-6} $Å^{-2}$). Because H_2O has a negative SLD, the total SLD of the film decreases as the water content in the nafion film increases with relative humidity as also shown by the shift in the critical edge to lower values from Figure 3. A large shift in the critical edge in liquid water compared to the vapor data is due to the fact that the incident medium of the neutrons in the liquid cell is a Si block as mentioned in the experimental section compared to the vapor cell where the incident medium is air.

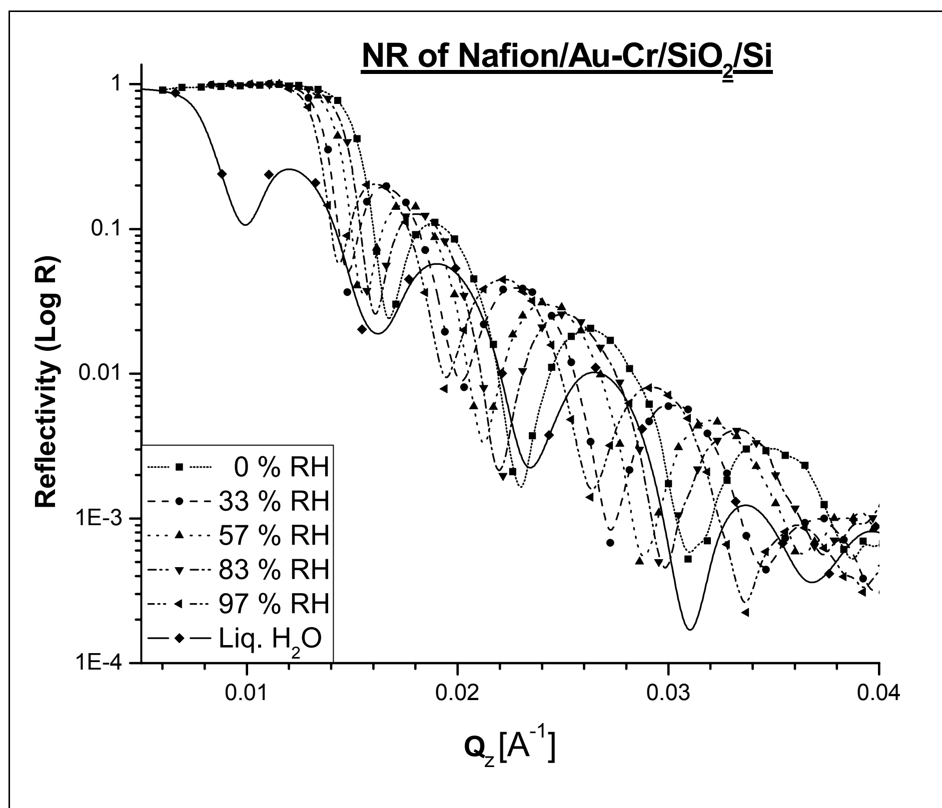

Figure 3. NR profiles for a thin nafion 1100 film spin coated on a Au-Cr/Si substrate at varying relative humidities. Sample temperature is 23 °C.

Figure 4 represents the simplest model one could propose for the nafion thin-film sample. It consists of Si as the incident medium (only 100 Å is shown), an oxide layer of

Si, a layer of chromium oxide, a chromium metal layer followed by a gold layer, and nafion. The thicknesses of the metallic region and the oxide layer have been refined, along with their SLD values and the widths of the interface regions. The chromium oxide layer beneath a chromium metal layer is indicative of the sputter source being contaminated with a thick oxide layer prior to deposition as Cr is known to oxidize readily.

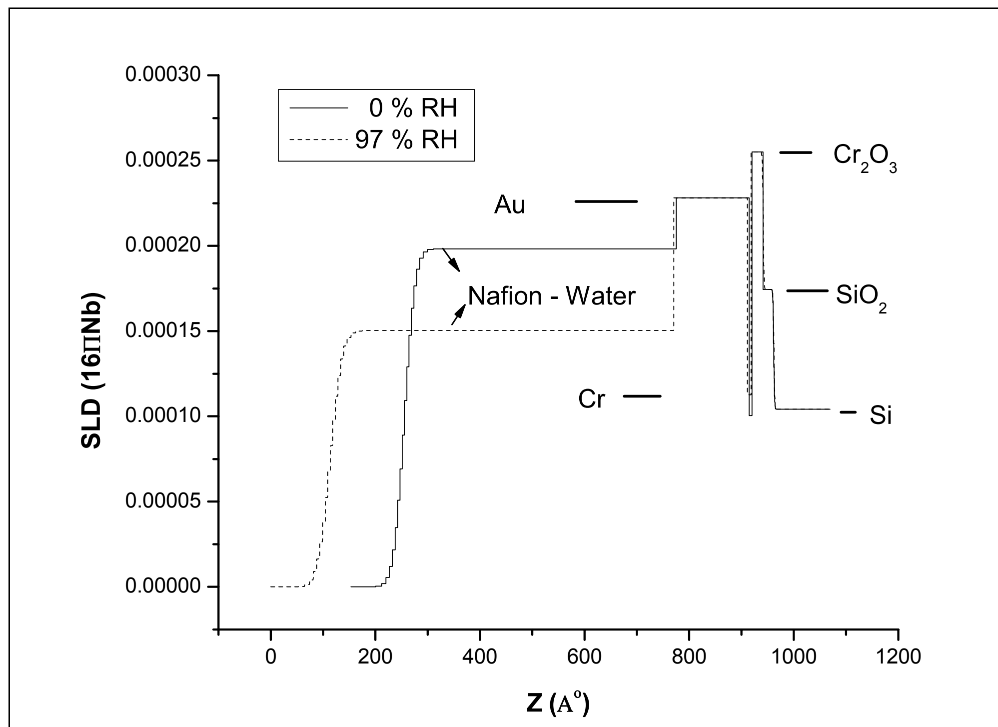

Figure 4. Least square fitted SLD profile of the nafion film at 0% and 97% RH. The numerical parameters of the model consisting of six distinct media, Si, SiO_2, Cr_2O_3, Cr, Au and Nafion are given in Table II. The gradual interfaces between layers are represented by hyperbolic tangent functions.

Table I is a list of scattering length densities of materials that are relevant to this sample along with their theoretical SLD. The initial bulk values of SLD for the substrate layers were allowed to vary during the least square fitting and it is possible that the layers were porous and the actual SLD values could be lower or higher depending on whether the pores remained vacant or were filled by species of different scattering length as shown. Any deviation in the SLD from its bulk value is also accompanied by variations in the surface roughness and thickness of that layer. The fitting methodology adopted takes into account these details before arriving at the best fit. Since the agreement is obtained by fitting the initial model there is a possibility that a different initial model would have given a better fit. Therefore, in analyzing reflectometry data, one always has to consider if the fitted model is reasonable. We took the approach that we would start with the simplest model, and no feature would be added unless it led to a significantly better fit, and made physical and chemical sense. Also, the SLD, thickness and roughness of the nafion layer in Table I is based on the least square fitted SLD model plotted in Figure 4 for the nafion film under dry (0% RH) and fully humidified (97% RH) conditions.

Table I. Numerical parameters for the least square fitted model representing the Nafion on the Au-Cr/Si substrate. The underlying layers of Au, Cr, Cr_2O_3 and SiO_2 were allowed to vary within acceptable limits to get best fits.

Layer	Theoretical SLD based on Bulk Density (x 10^{-4}) ($Å^{-2}$)	Scattering Length Density (x 10^{-4}) ($Å^{-2}$)	Thickness (Å)	Roughness (Å)
Nafion (Varying RH)	2.0925	1.9829 – 1.4013	519.94 – 681.51	32.28 – 43.65
Gold	2.2265	2.282	139 – 141	0 – 0.0043
Cr	1.5215	1.0034 – 1.1268	5.66 – 7.07	0
Cr2O3	2.5656	2.5504	20.76 – 23.13	0 – 0.005
SiO2	1.7436	1.7437	20.49 – 25.49	0 – 3.11
Si	1.0418	1.0418	100	3

The SLD along with the thickness and roughness of the Nafion layer for each RH, extracted from fitting the NR data using a multiple layer profile is given in Table II. A swelling ratio based on the thickness of the as prepared dry nafion film exemplifies the water uptake of the perfluoro sulfonic acid group with increasing humidity. The swelling ratio is calculated based on the increase in thickness of the nafion film as it hydrates compared to its dry thickness given by equation 2:

$$\text{Swelling ratio} = \frac{T_R - T_0}{T_0} \quad [2]$$

where T_R is the thickness at a given humidity and T_0 is the thickness of the dry film at 0% RH.

Table II. Summary of modeled properties for a thin Nafion 1100 EW film on Au-Cr/Si substrate at various %RH at 23 °C.

Relative Humidity (% RH)	Scattering Length Density (x 10^{-4})	Thickness (Å)	Roughness (Å)	Swelling ratio
Dry	1.9829	519.94	39.38	0
33	1.8187	549.74	32.28	0.0573
57	1.7208	578.07	33.51	0.1118
83	1.5755	625.28	35.20	0.2026
90	1.5795	637.22	36.71	0.2256
97	1.5033	656.87	43.65	0.2634
Liq. H_2O	1.4013	28.30	-	-
	1.4588	653.21	-	0.3107

Figure 5 shows the neutron reflectivity data obtained on the nafion thin-film on Au-Cr/Si substrate at 33%RH and the corresponding fit parameters based on the SLD profile illustrated in Figure 4 and Table II. The error in the fit parameters is due not only to the statistical uncertainties in the measured neutron reflectivity intensities, but also to the fact

that the reflectivity was collected over a finite range of Q. In spite of the uncertainties in the measured reflectivities the goodness-of-fit is well within acceptable limits.

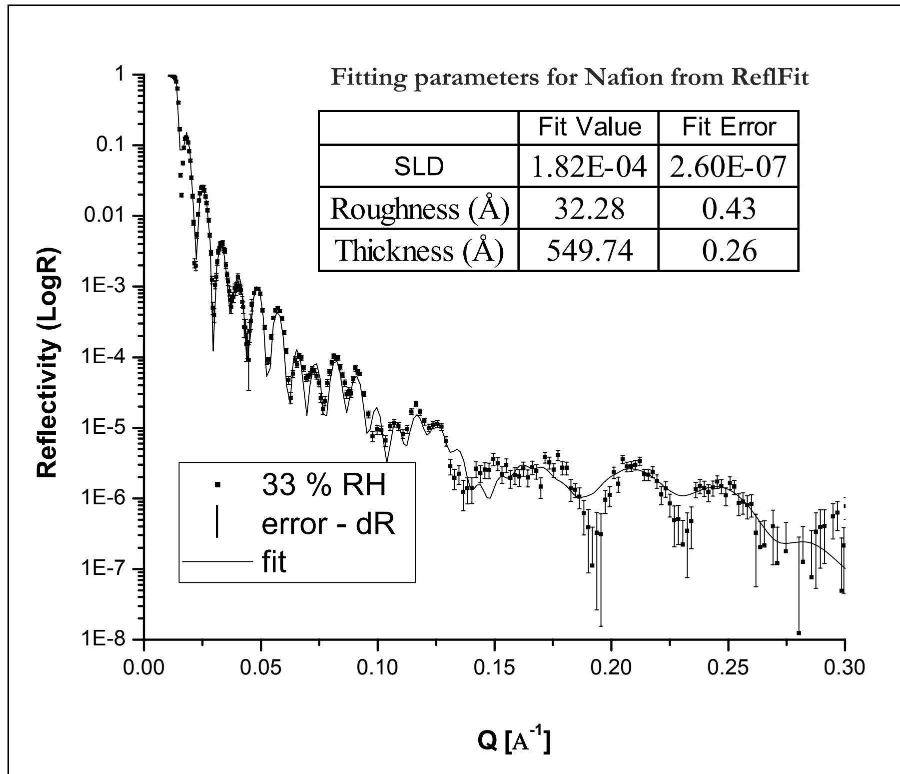

<u>Figure 5.</u> NR of the nafion film at 33% RH and the corresponding least square fit. Points are experimental data and solid line is the best fit. The underlying layers are based on the profile given in Table II.

Figure 6 shows the change in thickness of the nafion film as a function of relative humidity as given in Table II. The fits to the data in liquid water involved a less hydrophilic top surface and a more hydrophilic thin (~28 Å) inner layer. However, the swelling ratio in Table II is based on the total thickness of the nafion layer. The SLD of the 2 nafion layers, although slightly different from each other, are consistent with higher water content within the total nafion layer based on the higher total thickness and lower SLD compared to 97% RH vapor data.

The water uptake in nafion thin-film membranes are found according to equation 3:

$$\text{Water Uptake}\,(\lambda) = \text{Volume ratio of}\,\frac{\text{Nafion}}{H_2O} * \frac{V_{fract}}{1 - V_{fract}} \qquad [3]$$

where volume fraction of H_2O, $V_{fract} = \frac{(Nb_{Nafion} - Nb_{fit})}{(Nb_{Nafion} - Nb_{H2O})}$

Here, Nb_{nafion} is the theoretical SLD of Nafion (2.0925 x 10^{-4} x 16 pi), Nb_{H2O} is the theoretical SLD of liquid water and Nb_{fit} is the SLD derived from the fits of the data. The λ values hence derived from neutron reflectometry provide for a more accurate way of measuring the water uptake for nafion and similar membranes than traditional weight loss methods.

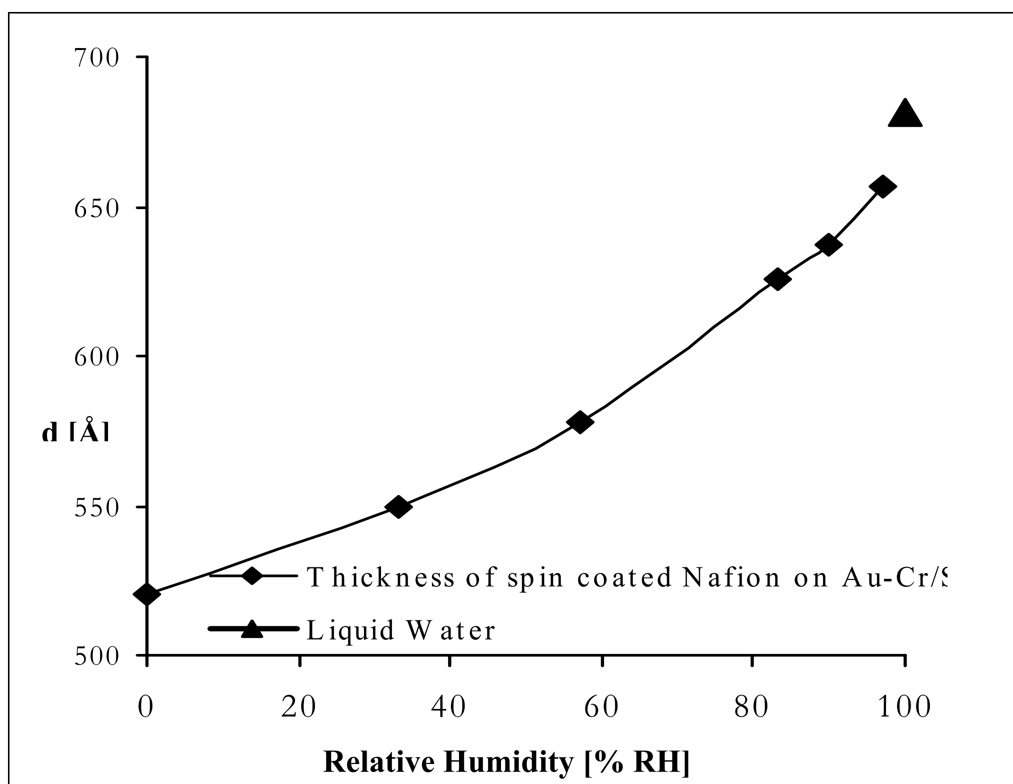

Figure 6. Thickness of the thin nafion 1100 EW film spin coated on a Au-Cr/Si substrate at varying relative humidities. Sample temperature is 23 °C. The total film thickness in liquid water is also included.

However, the water uptake,λ, in Table III for the nafion film at 97 % RH suggests that the nafion film is not completely humidified. The typical λ values reported in literature for nafion films at 100% RH from water vapor is 15. Further, the water uptake of nafion in the current study from liquid water is ~12 as compared to the literature value of 22.[30-33]

Table III. Summary of water uptake (λ), thickness and SLD for a thin Nafion 1100 EW film on Au-Cr/Si substrate at various %RH at 23 °C.

Relative Humidity (% RH)	Scattering Length Density (x 10-4)	Thickness (Å)	λ (based on SLD)
0	1.9829	519.94	1.5530
33	1.8187	549.74	4.1842
57	1.7208	578.07	5.9583
83	1.5755	625.28	8.9363
90	1.5795	637.22	8.8481
97	1.5033	656.87	10.5964
Liq. H_2O	1.4014	28.30	13.1828
	1.4588	653.21	11.6877

Water uptake of a separate sample of Nafion on a nominal thickness of 50 Å Pt/Si is also investigated using NR. The dry thickness of nafion film spin coated on Pt/Si from a diluted 5 wt.% Nafion 1100 EW is slightly larger (~ 80 Å) than the nafion films spin coated on the Au-Cr/Si under similar conditions. Whether the choice of substrate has an effect on the intrinsic bonding strength with Nafion thin films is the focus of future investigations and is not discussed in our current study. Prior to spin coating the nafion, the Pt/Si sample was characterized using X-ray reflectivity and the surface profile is plotted in Figure 7a along with the fits to the x-ray data (Figure 7b).

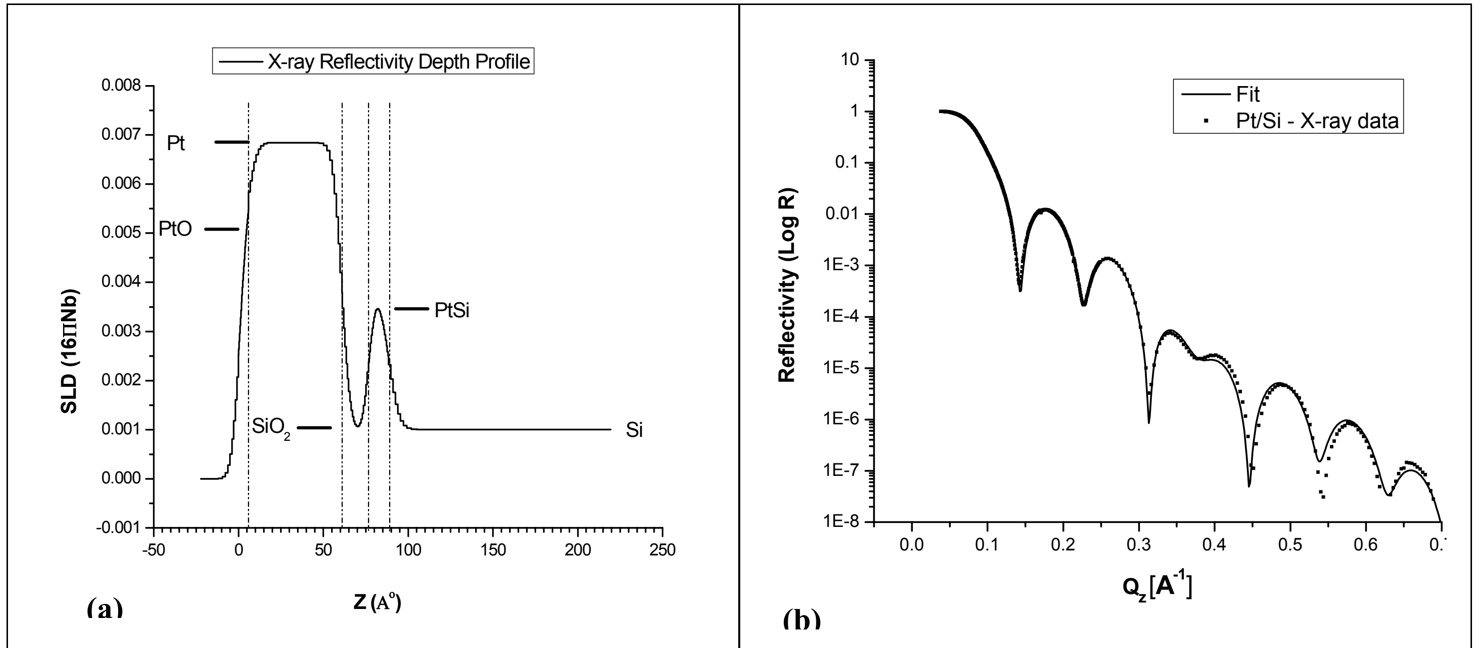

Figure 7. (a) Least square fitted x-ray SLD profile of the Pt/Si. Based on fitting (b), the model consists of five distinct media, Si, PtSi, SiO_2, Pt and PtO.

Based on the x-ray fitting a model consisting of Si (only 100 Å is shown), a platinum silicide layer, an oxide layer of Si, a platinum metal layer followed by a very thin PtO layer (<7 Å). Previous literature shows the presence of a silicide layer formed between the Si substrate and the native SiO_2 on similar sputtered Pt samples.[34] A model where the PtSi layer is placed above the SiO_2 layer does not give a reasonable fit to the data.

Figure 8 shows the NR data as a function of relative humidity from a nafion film deposited on a Pt/Si. The critical edge decreases as the water content in the nafion film increases with relative humidity similar to values from Figure 3. The inset in Figure 8 shows the reflectivity curve at 96% relative humidity over the entire range of θ (0.05°<θ<7°). The broad Q peaks above 0.15 $Å^{-1}$ are the interference fringes arising from the underlying Pt layer.

The SLD along with the thickness and water uptake of the Nafion layer for each RH extracted from fitting the NR data using a multiple layer profile is given in Table IV. The fits to the data in liquid water involved a less hydrophilic top surface and a more hydrophilic thin inner layer similar to that observed on the nafion on Au-Cr/Si sample.

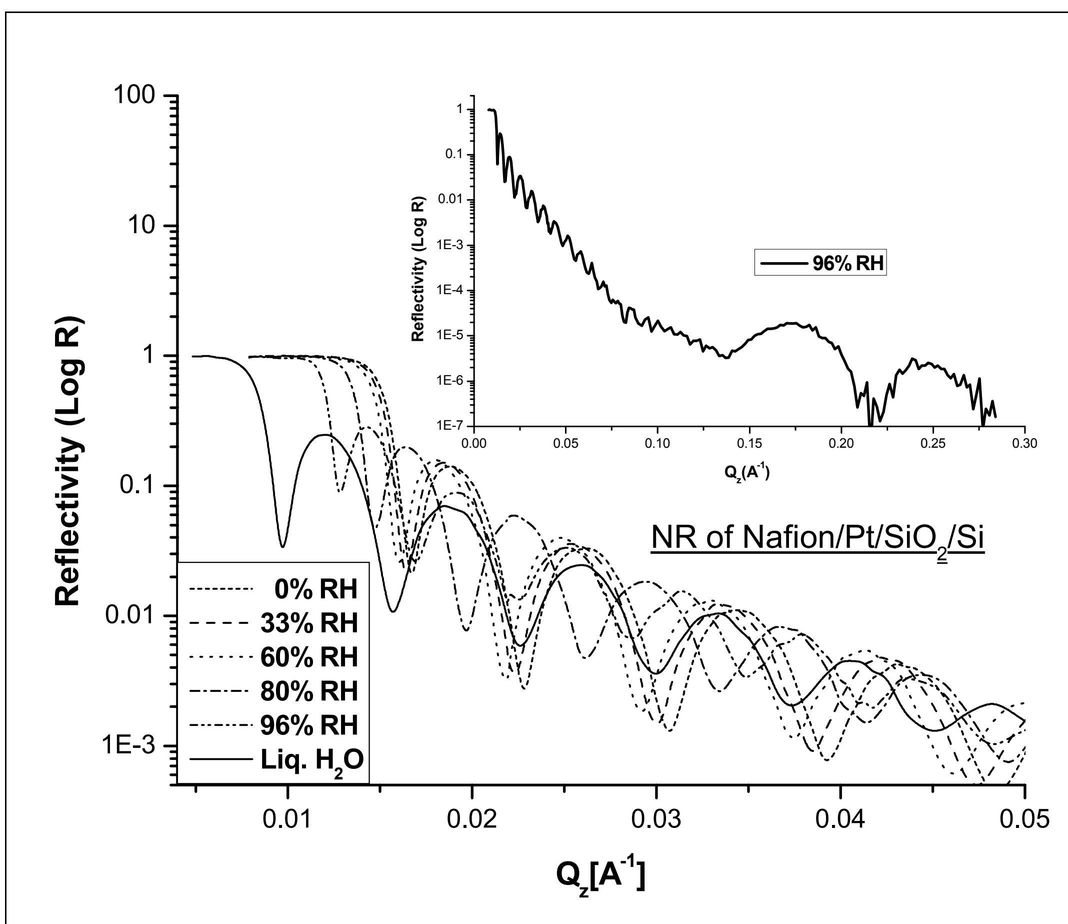

Figure 8. NR profiles for a thin nafion 1100 film spin coated on a Pt/Si substrate at varying relative humidities. Sample temperature is 23 °C.

Table IV. Summary of water uptake (λ), thickness and SLD for a thin Nafion 1100 EW film on Pt/Si substrate at various %RH at 23 °C.

Relative Humidity (% RH)	Scattering Length Density (x 10-4)	Thickness (Å)	λ (based on SLD)
0	2.0127	591.761	1.1160
33	1.9538	608.374	1.9907
60	1.8845	627.495	3.0814
80	1.6345	716.137	7.6734
96	1.2871	863.423	16.4802
Liq. H_2O	1.1538	16.06	20.9928
	1.5209	764.03	10.1797

The water uptake of the hydrophilic inner layer based on the SLD is ~21. However, the outer layer nafion contains only about 10 waters per sulfonic acid group. Even though the water content of the inner layer is more than that observed at 96% RH, the average λ

over the entire thickness of the nafion film is only 10.4. This is consistent with the lower total thickness of the nafion in liquid water. This result is in contrary to the water uptake observed in bulk nafion films where the λ value in liquid water is 22 as compared to 15 at 100% RH. Although the water uptake values averaged over the entire thickness of the nafion film reported in this manuscript are significantly lower than bulk films at near complete hydration in liquid water, at 100 % RH the λ values are comparable to those observed on bulk nafion films at the same humidity.[35] The non-zero λ values reported at 0% RH is a deviation from bulk like films where the nafion films are completely dry. However, this deviation may be a result of the nafion solution density values used to extract the water uptake from the scattering length densities. These spin coated nafion films might have a slightly different density than bulk films depending on the casting method and annealing temperatures.

One of the important observations based on the SLD of the nafion films on both Au-Cr and Pt is the presence of a thin hydrophilic layer (~15 – 30 Å) at the metal-nafion interfaces. This is in contrary to a previous report based on a similar NR technique, where an outer more hydrophilic layer and an inner less hydrophobhic layer of nafion on a Pt/GC (glassy carbon) substrate was reported.[36] They also proposed different multilayer models to describe the nafion 1100 EW films on different substrates. This is similar to the results observed in this study where the inner hydrophilic nafion layer on Pt and Au-Cr surfaces, based on water uptake from liquid water, yielded layers with significantly different thickness and λ values. Also, such a bilayer is not observed on nafion films under water vapor exposures even at 97% RH. Preliminary trials investigating thicker nafion membranes (~2000 Å) on Pt/Si showed that higher λ values similar to those observed on bulk membranes can be achieved depending on a multiple of variables, not shown here, including the kinetics of water sorption, heat treatment and thickness of the nafion film.

Although, all measurements in this report were performed at varying RH and in liquid water and were never exposed to an operating fuel cell condition i.e. electrochemical potential, current, oxygen or hydrogen gas, the SLD and thickness of the nafion films and hence their water uptake observed suggests that the nafion inonomer in the catalyst-PEM interface of a PEMFC membrane electrode assembly might differ in its physical properties compared to bulk nafion films depending on the nature of the surface it is in contact with. Hence, investigation of such interfaces (Nafion/Pt and Nafion/Au) using Neutron reflectometry are absolutely essential to (a) understand the nature of current state of the art polymer electrolyte membranes and (b) to provide as an advanced tool to support the development of new and durable membranes. Further, such interfaces serve as a model system to investigate the interface structures that form in the PEM near the catalyst electrodes in fuel cells in the three phase region where the PEM comes into contact with the elecrode/catalyst and the fuel or oxidizer.

Conclusions

In this report we have examined the water structure at the interface between Nafion and metal surfaces using Neutron Reflectometry. The results showed that spin-coated nafion films on Pt and Au surfaces may not have homogeneous density and hence the water content in these films may not be uniform. While the interfaces required for this techniques are in the form of 2-dimensional planes rather than the nanometer to

micrometer sized three dimensional particles used as additives, the water/Nafion structures observed here may also exist in the catalyst-ionomer-PEM three-phase interface. This has tremendous implications on the durability and mass transport properties of nafion in the catalyst layer of a PEMFC.

Finally, NR technique is a more accurate method of measuring water uptake due to the sensitivity of neutrons for hydrogen rich systems while providing structural information on the nanometer scale relevant to conventional fuel cell components. Also, in the future NR may become increasingly useful in understanding smaller scaled fuel cells. Therefore, fundamental studies are being conducted to establish the properties of spin cast PEM layers, for both utility in micron sized devices and for comparison to bulk materials.

Acknowledgements

We acknowledge the support extended by the NIST Center for Nanoscale Science and Technology (CNST) for the preparation of some of the sputtered samples.

*Certain commercial materials, instruments, and equipment are identified in this manuscript in order to specify the experimental procedure as completely as possible. In no case does such identification imply a recommendation or endorsement by the National Institute of Standards and Technology nor does it imply that the materials, instruments, or equipment identified is necessarily the best available for the purpose.

References

1. P. J. Ferreira, G. J. la O', Y. Shao-Horn, R. M. D. Morgan, S. Kocha and H. A. Gasteiger, *J. Electrochem. Soc.*, **152**, A2256 (2005).
2. J. Xie, D. L. Wood III, D. M. Wayne, T. A. Zawodzinski, P. Atanassov and R. L. Borup, *J. Electrochem. Soc.*, **152**, A104 (2005).
3. J. Xie, D. L. Wood III, K. L. More, P. Atanassov and R. L. Borup, *J. Electrochem. Soc.*, **152**, A1011 (2005).
4. R. J. Bellows, M. Y. Lin, M. Arif, A. K. Thompson and D. Jacobson, *J. Electrochem. Soc.*, **146**, 1099 (1999).
5. M. A. Hickner, N. P. Siegel, K. S. Chen, D. N. McBrayer, D. S. Hussey, D. L. Jacobson and M. Arif, *J. Electrochem. Soc.*, **153**, A902 (2006).
6. D. J. Ludlow, C. M. Calebrese, S. H. Yu, C. S. Dannehy, D. L. Jacobson, D. S. Hussey, M. Arif, M. K. Jensen and G. A. Eisman, *J. Power Sources*, **162**, 271 (2006).
7. F. Xu, O. Diat, G. Gebel and A. Morin, *J. Electrochem. Soc.*, **154**, B1389 (2007).
8. V. Barbi, S. S. Funari, R. Gehrke, N. Scharnagl and N. Stribeck, *Polymer*, **44**, 4853 (2003).
9. J. A. Elliot, S. Hanna, A. M. S. Elliott and G. E. Cooley, *Macromolecules*, **33**, 4161 (2000).
10. M. Fujimura, T. Hashimoto and H. Kawai, *Macromolecules*, **14**, 1309 (1981).
11. T. D. Gierke, G. E. Munn and F. C. Wilson, *J. Polym. Sci., Polym. Phys.*, **19**, 1687 (1981).
12. L. Rubatat, G. Gebel and O. Diat, *Macromolecules*, **37**, 7772 (2004).
13. J. C. Perrin, S. Lyonnard and F. Volino, *J. Phys. Chem. C*, **111**, 3393 (2007).
14. A. A. Pivovar and B. S. Pivovar, *J. Phys. Chem. B*, **109**, 785 (2005).
15. C. Heitner-Wirguin, *Polymer*, **20**, 371 (1979).

16. M. Ludvigsson, J. Lindgren and J. Tegenfeldt, *Electrochim. Acta*, **45**, 2267 (2000).
17. Y. Wang, Y. Kawano, S. R. Aubuchon and R. A. Palmer, *Macromolecules*, **36**, 1138 (2003).
18. K. W. Feindel, L. P. A. LaRocque, D. Starke, S. H. Bergens and R. E. Wasylishen, *J. Am. Chem. Soc.*, **126**, 11436 (2004).
19. Q. Chen and K. Schmidt-Rohr, *Macromolecules*, **37**, 5995 (2004).
20. M. Takasaki, K. Kimura, K. Kawaguchi, A. Abe and G. Katagiri, *Macromolecules*, **38**, 6031 (2005).
21. G. Gebel and O. Diat, *Fuel Cells*, **5**, 261 (2005).
22. G. Gebel and J. Lambard, *Macromolecules*, **30**, 7914 (1997).
23. M. Kim, C. J. Glinka, S. A. Grot and W. G. Grot, *Macromolecules*, **39**, 4775 (2006).
24. M. P. Seah, *et al.*, *Surf. Interface Anal.*, **36**, 1269 (2004).
25. J. A. Dura, C. A. Richter, C. F. Majkrzak and N. V. Nguyen, *Appl. Phys. Lett.*, **73**, 2131 (1998).
26. S. Krueger, C. W. Meuse, C. F. Majkrzak, J. A. Dura, N. F. Berk, M. Tarek and A. L. Plant, *Langmuir*, **17**, 511 (2001).
27. P.A. Kienzle, K.V. O'Donovan, J.F. Ankner, N.F. Berk and C. F. Majkrzak, http://www.ncnr.nist.gov/reflpak (2000-2006).
28. L. G. Parratt, *Phys. Rev.*, **95**, 359 (1954).
29. J. A. Dura, *et al.*, *Rev. Sci. Instr.*, **77**, 074301/1 (2006).
30. L. Zhang, C. S. Ma and S. Mukerjee, *Electrochim. Acta*, **48**, 1845 (2003).
31. T. A. Zawodzinski, T. E. Springer, J. Davey, R. Jestel, C. Lopez, J. Valerio and S. Gottesfeld, *J. Electrochem. Soc.*, **140**, 1981 (1993).
32. T. A. Zawodzinski, C. Derouin, S. Radzinski, R. J. Sherman, V. T. Smith, T. E. Springer and S. Gottesfeld, *J. Electrochem. Soc.*, **140**, 1041 (1993).
33. L. Zhang, C. S. Ma and S. Mukerjee, *Electrochimica Acta*, **48**, 1845 (2003).
34. D. M. Solina, R. W. Cheary, P. D. Swift, S. Dligatch, G. M. McCredie, B. Gong and P. Lynch, *Thin Solid Films*, **372**, 94 (2000).
35. P. Choi, N. H. Jalani and R. Datta, *J. Electrochem. Soc.*, **152**, E84 (2005).
36. D. L. Wood, J. Chlistunoff, E. B. Watkins, P. Ataanassov and R. L. Borup, *ECS Transactions*, **3**, 1011 (2006).